Translational invariant parent Hamiltonians of valence bond crystals

D. Huerga,[1,*] A. Greco,[2] C. Gazza,[2] and A. Muramatsu[1]

[1] *Institut für Theoretische Physik III, Universität Stuttgart, Pfaffenwaldring 57, D-70550 Stuttgart, Germany*

[2] *Universidad Nacional de Rosario and Instituto de Física Rosario, CONICET, Bv. 27 de Febrero 210bis, S2000EZP Rosario, Argentina*

We present a general method to construct translational invariant and SU(2) symmetric antiferromagnetic parent Hamiltonians of valence bond crystals (VBC). The method is based on a canonical mapping transforming S=1/2 spin operators into a bilinear form of a new set of *dimer fermion* operators. We construct parent Hamltonians of the columnar- and the staggered-VBC on the square lattice, for which the VBC is an eigenstate in all regimes and the exact ground state in some region of the phase diagram. We study the depart from the exact VBC regime upon tuning the anisotropy by means of the hierarchical mean field theory and exact diagonalization on finite clusters. In both Hamiltonians, the VBC phase extends over the exact regime and transits to a columnar antiferromagnet (cAF) through a window of intermediate phases, revealing an intriguing competition of correlation lengths at the VBC-cAF transition. The method can be readily applied to construct other VBC parent Hamiltonians in different lattices and dimensions.

arXiv:1611.07893v1 [cond-mat.str-el] 23 Nov 2016

Quantum magnets, characterized by the complex interplay between interactions among the electrons' spin and the lattice geometry, host a wealth of phases and exotic phenomena. Particularly interesting is the transition from a disordered –*quantum paramagnetic*– phase to an ordered antiferromagnetic (AF) phase at zero temperature through a quantum phase transition [1], which can be experimentally probed by applying external pressure [2] or magnetic field [3]. One particular type of such quantum paramagnetic phases is the valence bond crystal (VBC), characterized by the "dimerization" of the system in spin-singlets (valence bonds) in a periodic pattern usually breaking the translational symmetry of the lattice. Under certain specific conditions, it has been argued that a class of VBC-AF transitions in two-dimensions (2D) are driven by the deconfinement of fractional excitations at a critical point [4], contrary to what is generally expected within Landau theory. To test these ideas, a family of antiferromagnetic Heisenberg Hamiltonians with additional four- and six-spin interactions favoring VBC order and amenable to quantum Monte Carlo (QMC) computations have been introduced during the last decade [5–7]. These models, so-called J-Q models, show unusual scaling behavior at the VBC-AF transition point [7–11] and, in some cases, a weak VBC signal [5, 8]. In order to furnish this putative new class, it would be desirable to enlarge the number of Hamiltonians hosting VBC-AF transitions. In particular, antiferromagnetic Hamiltonians hosting an *exact* VBC groundstate (GS) shall provide a convenient test bed where the VBC phase is unambiguously defined.

Existing parent Hamiltonians of VBC states are a few, being the paradigmatic models in 1D and 2D the Majumdar-Gosh [12] and Shastry-Sutherland [13] models, respectively. More recently, 2D parent Hamiltonians of different VBCs have been constructed [14–16] by using sums of local projectors [17]. However, this method may lead to a GS manifold of various degenerate VBC patterns.

In this work, we present a general method to construct SU(2) symmetric and translational invariant VBC parent Hamiltonians based on a canonical mapping that exactly identifies a VBC state –i.e. a product of singlets– with the vacuum of a new set of *dimer fermions* (DF). Starting with a generic anisotropic AF Heisenberg Hamiltonian as an Ansatz, this mapping guides our search for additional translational invariant interactions that, summed to the Ansatz, make the vacuum to be an exact eigenstate of the sum. As an example, we construct parent Hamiltonians of the staggered- and the columnar-VBC (sVBC and cVBC) on the square lattice, finding that anisotropic four-spin interactions are required to exactly stabilize the VBC in both cases. Interestingly, the sVBC parent Hamiltonian hosts an exact GS within a finite region of the phase diagram, differently from other parent Hamiltonians where the exact GS is found on a single point [12, 14–16]. Upon tuning the anisotropy, the VBC transits to a columnar AF (cAF) phase characterized by a finite magnetization at the columnar wave vector $(0, \pi)$ through a window of intermediate phases (IPs) characterized by the strong competition of correlations at different characteristic lengths (see Fig. 1).

Dimer fermion mapping.—Consider a lattice where a quantum spin S=1/2, described by the operator S_j^a $(a = x, y, z)$, resides on each vertex, j, of a lattice of size $\mathcal{N}$. We choose a VBC pattern on this lattice, defining a superlattice where in each vertex, r, resides a dimer, i.e. a pair of nearest-neighbor (NN) spins. Each site of the lattice can thus be referred to by its position within a dimer, α, and the position of the dimer in the superlattice, i.e. $j \equiv r, \alpha$ $(\alpha = 1, 2)$. Considering the Majorana representation of spins [18], $S_j^a = -\frac{\mathrm{i}}{2}\sum_{b,c}\varepsilon^{abc}\eta_j^b\eta_j^c$, where ε^{abc} is the Levi-Civita tensor and the Majorana fermions, $\eta_j^a = \eta_j^{a\dagger}$, obey anticommutation relations

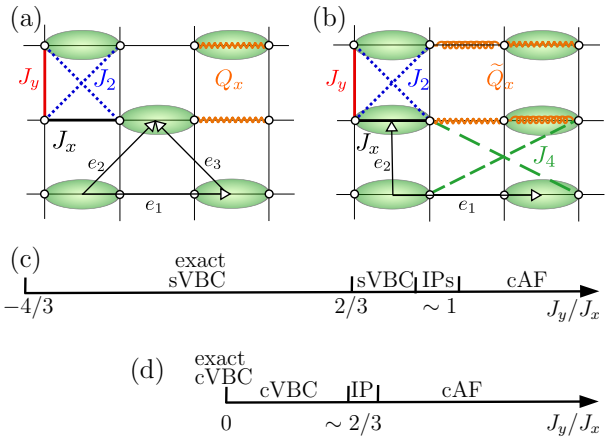

FIG. 1. (Color online) Schematic representation of the sVBC (a) and cVBC (b) states and their respective parent Hamiltonians, together with their phase diagrams, (c) and (d). Green ovals represent dimers, thick solid lines represent the Heisenberg interaction among NN spins along the x (black) and y (red) directions, second-NN spins (dotted blue), and a subset of fourth-NN spins (dashed green). Pairs of orange waved- and spring-lines represent anisotropic four-spin interactions.

$\{\eta_i^a, \eta_j^b\} = \delta^{ab}\delta_{ij}$, we define a *dimer fermion* (DF) as the linear combination of two Majorana fermions of a dimer,

$$f_r^{a\dagger} = \frac{1}{\sqrt{2}}\left(\eta_{r,1}^a + \mathrm{i}\eta_{r,2}^a\right), \quad f_r^a = (f_r^{a\dagger})^\dagger. \tag{1}$$

The DFs obey the usual fermionic anticommutation relations, $\{f_r^a, f_{r'}^{b\dagger}\} = \delta^{ab}\delta_{rr'}$. Inverting the relation (1), we can express the spin operators in terms of DFs,

$$S_{r,1}^a = \frac{1}{2}\sum_{b,c}\varepsilon^{abc}\left(T_r^{bc} + \Delta_r^{bc}\right), \tag{2}$$

$$S_{r,2}^a = \frac{1}{2}\sum_{b,c}\varepsilon^{abc}\left(T_r^{bc} - \Delta_r^{bc}\right), \tag{3}$$

where we have defined the fully antisymmetric number-conserving and non-conserving DF operators,

$$T_r^{ab} = -\frac{\mathrm{i}}{2}\left(f_r^{a\dagger}f_r^b - f_r^{b\dagger}f_r^a\right), \tag{4}$$

$$\Delta_r^{ab} = -\frac{\mathrm{i}}{2}\left(f_r^{a\dagger}f_r^{b\dagger} - f_r^b f_r^a\right). \tag{5}$$

The operators (4) and (5) are indeed the generators of the SU(2)⊗SU(2)≃SO(4) algebra of a dimer [19]. Notice that the mapping (2)-(3) relating S=1/2 spin operators and DFs is canonical without the need of any additional constraint, contrary to other slave-particle mappings.

In the DF representation, the dimer Hilbert space is doubled with respect the physical one, existing two equivalent copies of the singlet ($|s\rangle$) and the triplet states. By applying the total spin operator, $\mathbf{S}_r^2 = (\mathbf{S}_{r,1} + \mathbf{S}_{r,2})^2$, and its third component, $S_r^z = (S_{r,1}^z + S_{r,2}^z)$, to the eight DF states of the dimer we can identify the vacuum and double occupied DF states, on the one hand, and the fully and single occupied states, on the other, with two equivalent copies of the singlet and triplet states (see Supplemental Material for details on the dimer fermion mapping). Without loss of generality, the VBC state can be identified with the DF vacuum,

$$|\mathrm{VBC}\rangle = \prod_r |s\rangle_r = |0\rangle. \tag{6}$$

A direct consequence of the DF mapping (2)-(3) is that the Heisenberg (HB) interaction among two spins, $B_{ij} = \mathbf{S}_i\mathbf{S}_j$, maps to a one-body DF operator,

$$D_r = -\frac{3}{4} + \frac{1}{2}n_r(3 - n_r), \tag{7}$$

where $n_r = \sum_a f_r^{a\dagger}f_r^a$, when it acts on the two spins comprising a dimer ($i = r, 1$; $j = r, 2$). Alternatively, B_{ij} maps to a two-body DF operator when it acts on two different dimers ($i \in r$, $j \in r' \neq r$),

$$C_{rr'}^{\alpha\alpha'} = \frac{1}{2}\sum_{a,b}(T_r^{ab}T_{r'}^{ab} + V^{\alpha\alpha'}T_r^{ab}\Delta_{r'}^{ab} + V^{\alpha'\alpha}\Delta_r^{ab}T_{r'}^{ab} + W^{\alpha\alpha'}\Delta_r^{ab}\Delta_{r'}^{ab}), \tag{8}$$

where $V^{\alpha\alpha'}$ and $W^{\alpha\alpha'}$ refer to the elements of the 2×2 matrices,

$$V = \begin{pmatrix} 1 & -1 \\ 1 & -1 \end{pmatrix} \quad \text{and} \quad W = \begin{pmatrix} 1 & -1 \\ -1 & 1 \end{pmatrix},$$

encoding the information about the position of the two spins within their respective dimers.

VBC parent Hamiltonian construction.— Once chosen a VBC on a lattice determining a dimer tiling, we propose a general SU(2) symmetric AF ansatz Hamiltonian, H_0. For the sake of simplicity, let us restrict in the following to the construction of the sVBC on the square lattice, although the same steps can be followed in other cases. In this case,

$$H_0 = \sum_j\left(J_x B_{j,j+\hat{x}} + J_y B_{j,j+\hat{y}}\right). \tag{9}$$

where we refer by $\hat{x}$ and $\hat{y}$ to the unit vectors defining the square lattice. We rewrite (9) in terms of DFs by directly applying the DF mapping (2)-(3),

$$H_0^{\mathrm{DF}} = J_x\sum_r\left(D_r + C_{r,r+e_1}^{21}\right) + J_y\sum_r\left(C_{r,r+e_2}^{21} + C_{r,r+e_3}^{12}\right), \tag{10}$$

where e_1, e_2 and e_3 refer to the basis vectors of the triangular superlattice defined by the sVBC (Fig.1).

The terms preventing the DF vacuum to be an eigenstate of (10) are the $\Delta\Delta$ terms of the inter-dimer operators (8), as $C_{rr'}^{\alpha\alpha'}|0\rangle = W^{\alpha\alpha'}\sum_{a,b}\Delta_r^{ab}\Delta_{r'}^{ab}|0\rangle$. Therefore, we need to search for *additional* translational invariant

and SU(2) symmetric terms ($H_{\rm ad}$) such that they annihilate the $\Delta\Delta$ terms in (10), and make the DF vacuum to be an eigenstate of the total Hamiltonian, $H = H_0 + H_{\rm ad}$, with eigenvalue $\varepsilon = -3J_x\mathcal{N}/8$. In constructing $H_{\rm ad}$, we make use of the symmetry properties of the inter-dimer operator (8),

$$C^{11}_{rr'}\left|0\right\rangle = C^{22}_{rr'}\left|0\right\rangle = -C^{12}_{rr'}\left|0\right\rangle = -C^{21}_{rr'}\left|0\right\rangle . \qquad (11)$$

In particular, by adding a second-NN Heisenberg term, $J_2\sum_{\langle\langle ij\rangle\rangle} B_{ij}$, with $J_2 = J_y/2$, we can annihilate the $\Delta\Delta$ terms along the e_2 and e_3 directions of the triangular superlattice (see Fig. 1). The remaining $\Delta\Delta$ terms along the e_1 direction can be annihilated by adding an anisotropic four-spin interaction, $Q_x\sum_{\langle ijkl\rangle} B_{ij}B_{kl}$, with $Q_x = 2J_x/3$, where $\langle ijkl\rangle$ refers to a plaquette of the square lattice. Finally, the sVBC is then an eigenstate of

$$H = \sum_j \left(J_x B_{j,j+\hat{x}} + J_y B_{j,j+\hat{y}}\right) + \frac{J_y}{2}\sum_{\langle\langle ij\rangle\rangle} B_{ij} + \frac{2J_x}{3}\sum_{\langle ijkl\rangle} B_{ij}B_{kl}. \qquad (12)$$

In order to assess whether the DF vacuum is not just an eigenstate but the exact GS in any regime, the total Hamiltonian is expressed as a translational invariant sum of local Hamiltonians shifted by the DF vacuum eigenvalue, i.e. $H = \varepsilon + \sum_j H_j$. The local Hamiltonian of (12) is straightforward and thus given in the Supplemental Material. If the local Hamiltonian H_j is semi-positive definite, the DF vacuum is the exact GS. In particular, the sVBC is the exact GS of (12) within the range $-4/3 \leq J_y/J_x \leq 2/3$.

Notice that alternatively to the four-spin interaction, we may have added a second-NN HB interaction along the x-direction to annihilate the $\Delta\Delta$ terms along the e_1 direction. However, the resulting local Hamiltonian is not semi-definite positive.

Following the same steps, one can show that the cVBC is the exact GS of

$$H = \sum_j \left(J_x B_{j,j+\hat{x}} + J_y B_{j,j+\hat{y}}\right) + J_2\sum_{\langle\langle ij\rangle\rangle} B_{ij} + J_4\sum_{\langle\langle\langle ij\rangle\rangle\rangle} B_{ij} + \widetilde{Q}_x\sum_{\langle ijkl\rangle} B_{ij}B_{kl}, \qquad (13)$$

for the particular point $J_y = 0$, when the couplings are fixed to $J_2 = J_y$, $J_4 = J_y/2$, and $\widetilde{Q}_x = J_x/3$, and where the third term accounts for HB interactions among fourth-NN spins, and the fourth term accounts for four-spin interactions in tilted plaquettes (see Fig. 1).

Phase diagram.— As the sVBC and cVBC parent Hamiltonians are strongly frustrated, we study the depart from the exact VBC GS by combining exact diagonalization (ED) on finite clusters with periodic boundary conditions and hierarchical mean field theory (HMFT) in the Gutzwiller approximation [20–22]. From the technical standpoint, both methods involve the diagonalization of finite clusters of N sites, and their combined use provide complementary information about the thermodynamic limit.

The HMFT-Gutzwiller approach consists in using an homogeneus product of cluster wave functions as an Ansatz for the GS in the thermodynamic limit. Its variational determination reduces to perform ED on a cluster with open boundary conditions and a set of self-consistently defined mean-fields acting on its boundaries, which allow for the breakdown of symmetries and stabilization of different long-range orders. As a consequence, the sizes attained with HMFT are smaller than with ED. For appropriate choices of the cluster shape –romboid for the sVBC, and square for the cVBC– the HMFT wave function contains the exact VBC wave functions. In addition, it allows for the systematic computation of observables directly in the thermodynamic limit. In particular, the energy is an upper bound to the exact one. We characterize VBC and cAF phases by computing the magnetization $M_{\mathbf{k}} = \frac{1}{N}\sum_j e^{i\mathbf{k}\mathbf{r}_j}\langle S^z_j\rangle$, at different wave vectors and the dimerization along the x and y directions, $\mathcal{D}_\nu = \frac{1}{N}\sum_j (-1)^{j_\nu}\langle S_j S_{j+\hat{\nu}}\rangle$, where $\nu = x, y$ [1].

Upon tuning the anisotropy in the antiferromagnetic regime, we find for both Hamiltonians (12) and (13) that the VBC phase extends beyond the exact GS regime and transits to a cAF phase characterized by a vanishing singlet-triplet gap (ED) consistent with a strong columnar magnetization $M_{(0,\pi)} \sim 0.4$ (HMFT) through a region where various IPs appear when using large cluster sizes (HMFT) (see Figs. 2 and 3). In particular, in Fig.2 we show the scaling of the GS phase diagram of the sVBC parent Hamiltonian (12) as computed with ED ($N = 8, 16, 32, 36$) and HMFT ($N = 4, 8, 16, 24$), together with HMFT results on energies and order parameters (M and $\mathcal{D}$). The sVBC phase extends beyond the exact VBC regime both with ED (Fig.2a) and HMFT (Fig.2b). Within HMFT and small cluster sizes ($N = 4, 8$) we find a direct first order transition from the sVBC to the cAF phase. For bigger cluster sizes ($N = 16, 24$), the direct sVBC-cAF transition is replaced by a window of IPs: one within 16-HMFT and two (IP1 and IP2) within 24-HMFT. Interestingly, the IPs energies tend to smoothen the intersection of the sVBC and cAF linear energies found with smaller clusters (Fig.2c). The IP1 is characterized by suppression of dimer order, $\mathcal{D}_x \simeq -0.16$ (Fig.2d) while the IP2 is characterized by suppression of columnar magnetization. These IPs are numerically converged only when restricting the variational space to cluster configurations with $\sum_j \langle S^z_j\rangle = 0$. Moreover, the transition IP2-cAF takes place at a tiny region not fully converged even with this cutoff.

In Fig. 3 we show the scaling of the GS phase diagram of the cVBC parent Hamiltonian (13) as computed with ED ($N = 8, 16, 32$) and HMFT ($N = 4, 16, 24$) ob-

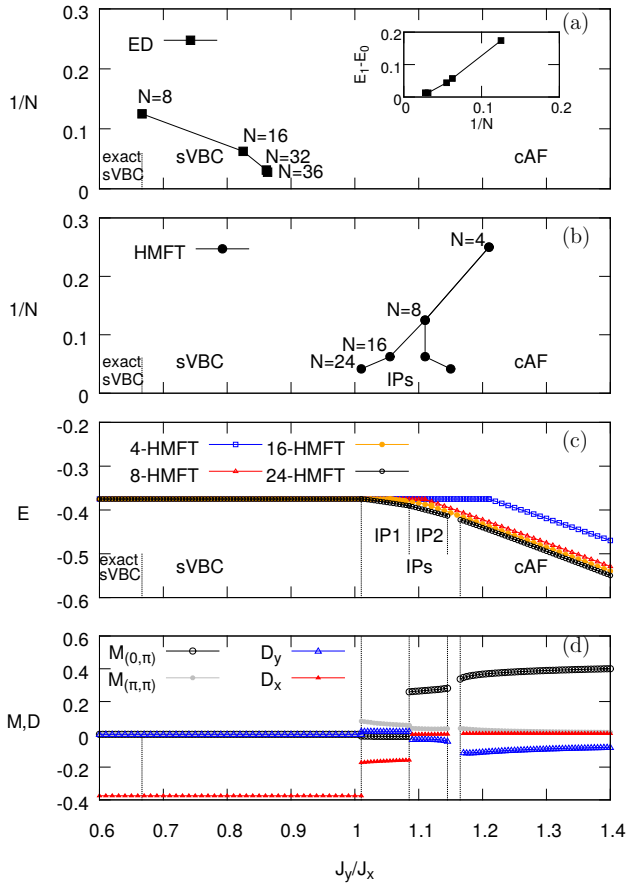

FIG. 2. (Color online) Scaling of the GS phase diagram of the sVBC parent Hamiltonian (12) as computed with (a) ED and (b) HMFT. Inset (a): Singlet-triplet gap computed with ED at $J_y/J_x = 1.4$. (c) Energy per site (units of J_x) computed with HMFT for different cluster sizes of romboid shape. (d) Magnetization M and dimerization $\mathcal{D}$ as computed with 24-HMFT.

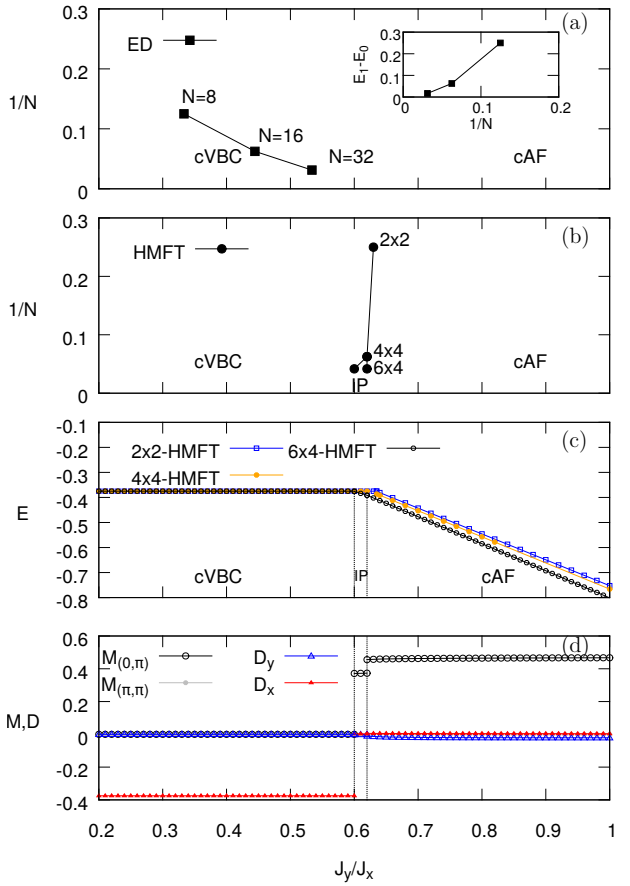

FIG. 3. (Color online) Scaling of the GS phase diagram of the cVBC parent Hamiltonian (13) as computed with (a) ED and (b) HMFT. Inset (a): Singlet-triplet gap computed with ED at $J_y/J_x = 1$. (c) Energy per site (units of J_x) computed with HMFT for different cluster sizes of square shape. (d) Magnetization M as computed with 6×4-HMFT.

taining a similar picture to the sVBC parent Hamiltonian phase diagram. Nevertheless, in this case a single IP with slightly suppressed cAF order an negligible dimerization appears in a small window when computing with the largest cluster available, 6×4-HMFT, suggesting that further IPs may eventually appear for greater cluster sizes. Same as for the sVBC parent Hamiltonian, this IP is only converged by applying the previously described cutoff of the variational space.

Summary and conclusion.—We have presented a systematic method to construct translational invariant SU(2) symmetric parent Hamiltonians of VBC states. The method is based on a canonical mapping identifying a VBC state with the vacuum of a new set of dimer fermions (DFs). This mapping guides our search for translational invariant interactions that added to an anisotropic AF Heisenberg Hamiltonian render the VBC to be an exact eigenstate, and the exact GS when the related local Hamiltonian is semi-positive definite. As an example, we have constructed the parent Hamiltonians of a staggered- and a columnar-VBC (sVBC and cVBC) on the square lattice, both requiring the explicit breakdown of the original C_4 symmetry of the lattice. A similar phase diagram is obtained for both Hamiltonians, where ED and HMFT computations show consistent results. The VBC extends over the exact regime and transits to columnar AF (cAF) through a window of intermediate phases (IPs) that appears when using large clusters. These IP window is characterized by the strong competition of correlations with characteristic length scales that possibly exceed the cluster sizes used, as revealed by their subtle numerical convergence, and may be replaced by an infinite series of first order transitions or even a continuous transition in the thermodynamic limit. The method here proposed can be readily used to construct VBC parent Hamiltonians on other lattices, such as the kagome

or honeycomb, for which various Hamiltonians with competing VBC states exist.

We gratefully acknowledge J. Riera for providing us with exact diagonalization codes. We acknowledge useful discussions with Adriana Foussats, Jorge Dukelsky, Gerardo Ortiz, Sumiran Pujari, Hui Shao, and Anders Sandvik. DH acknowledges computing time at JURECA, Jülich supercomputing center. CG acknowledges support from CONICET-PIPI0389. AG acknowledges support from CONICET-PIP0375. We devote this paper to the memory of Prof. Dr. Alejandro Muramatsu, who died before this work was completed. Alejandro initiated this work developping the main ideas and formalism. We will miss him, his physics and friendship.

* huerga@itp3.uni-stuttgart.de

[1] Sachdev Subir, Nat. Phys. **4**, 173 (2008).
[2] C. Rüegg, B. Normand, M. Matsumoto, A. Furrer, D. F. McMorrow, K. W. Krämer, H. U. Güdel, S. N. Gvasaliya, H. Mutka, and M. Boehm, Phys. Rev. Lett. **100**, 205701 (2008).
[3] V. Zapf, M. Jaime, and C. D. Batista, Rev. Mod. Phys. **86**, 563 (2014).
[4] T. Senthil, L. Balents, S. Sachdev, A. Vishwanath, and M. P. A. Fisher, Phys. Rev. B **70**, 144407 (2004).
[5] A. W. Sandvik, Phys. Rev. Lett. **98**, 227202 (2007).
[6] J. Lou, A. W. Sandvik, and N. Kawashima, Phys. Rev. B **80**, 180414 (2009).
[7] S. Pujari, K. Damle, and F. Alet, Phys. Rev. Lett. **111**, 087203 (2013).
[8] F.-J. Jiang, M. Nyfeler, S. Chandrasekharan, and U.-J. Wiese, Journal of Statistical Mechanics: Theory and Experiment **2008**, P02009 (2008).
[9] A. W. Sandvik, Phys. Rev. Lett. **104**, 177201 (2010).
[10] K. Chen, Y. Huang, Y. Deng, A. B. Kuklov, N. V. Prokof'ev, and B. V. Svistunov, Phys. Rev. Lett. **110**, 185701 (2013).
[11] H. Shao, W. Guo, and A. W. Sandvik, Science **352**, 213 (2016).
[12] C. K. Majumdar and D. K. Ghosh, Journal of Mathematical Physics **10**, 1388 (1969).
[13] B. S. Shastry and B. Sutherland, Physica B+C **108**, 1069 (1981).
[14] C. D. Batista and S. A. Trugman, Phys. Rev. Lett. **93**, 217202 (2004).
[15] B. Kumar, Phys. Rev. B **71**, 174434 (2005).
[16] A. Gellé, A. M. Läuchli, B. Kumar, and F. Mila, Phys. Rev. B **77**, 014419 (2008).
[17] D. J. Klein, Journal of Physics A: Mathematical and General **15**, 661 (1982).
[18] A. M. Tsvelik, Phys. Rev. Lett. **69**, 2142 (1992).
[19] A. Foussats, A. Greco, and A. Muramatsu, Nuclear Physics B **842**, 225 (2011).
[20] L. Isaev, G. Ortiz, and J. Dukelsky, Phys. Rev. B **79**, 024409 (2009).
[21] D. Huerga, J. Dukelsky, N. Laflorencie, and G. Ortiz, Phys. Rev. B **89**, 094401 (2014).
[22] D. Huerga, S. Capponi, J. Dukelsky, and G. Ortiz, Phys. Rev. B **94**, 165124 (2016).

Supplemental Material

THE DIMER FERMION MAPPING

The vacuum and doubly occupied DF states, and the fully and singly occupied DF states, comprise two equivalent copies of the dimer Hilbert space. We can classify them by applying the total spin, $\mathbf{S}_r^2 = (\mathbf{S}_{r,1} + \mathbf{S}_{r,2})^2$, and third component, $S_r^z = (S_{r,1}^z + S_{r,2}^z)$, written in terms of DFs to each of the eight fermionic states of a dimer.

The total spin of a dimer is,

$$\mathbf{S}_r^2 = 2\mathbf{S}_{r,1}\mathbf{S}_{r,2} + \mathbf{S}_{r,1}^2 + \mathbf{S}_{r,2}^2, \tag{S1}$$

The first term of the right-hand side is indeed twice the intra-dimer Heisenberg (HB) interaction, $D_r = \mathbf{S}_{r,1}\mathbf{S}_{r,2}$, which can be written in terms of DFs by directly applying the mapping (2)-(3),

$$\mathbf{S}_{r,1}\mathbf{S}_{r,2} = \frac{1}{4}\sum_a \sum_{b,c} \sum_{b',c'} \varepsilon^{abc}\varepsilon^{ab'c'} \left(T_r^{bc} + \Delta_r^{bc}\right)\left(T_r^{bc} - \Delta_r^{bc}\right). \tag{S2}$$

Taking into account the properties of the Levi-Civita tensor, $\sum_a \varepsilon^{abc}\varepsilon^{ab'c'} = \delta^{bb'}\delta^{cc'} - \delta^{bc'}\delta^{cb'}$, that $T_r^{bc}\Delta_r^{bc} = 0 = \Delta_r^{bc}T_r^{bc}$, and using the antisymmetry properties of the T (4) and Δ (5) DF operators,

$$\mathbf{S}_{r,1}\mathbf{S}_{r,2} = \frac{1}{2}\sum_{b\neq c} \left(T_r^{bc}T_r^{bc} - \Delta_r^{bc}\Delta_r^{bc}\right). \tag{S3}$$

Substituting the number conserving (T) and non-conserving (Δ) operators in terms of DFs and making use of the anticommutation relation of DFs,

$$\mathbf{S}_{r,1}\mathbf{S}_{r,2} = -\frac{1}{8}\sum_{b\neq c}\left[1 - 2\left(f_r^{b\dagger}f_r^b + f_r^{c\dagger}f_r^c\right)\right] - \frac{1}{2}\sum_{b\neq c} f_r^{b\dagger}f_r^b f_r^{c\dagger}f_r^c. \tag{S4}$$

Finally, taking into account the three fermionic species,

$$\mathbf{S}_{r,1}\mathbf{S}_{r,2} = -\frac{3}{4} + \frac{1}{2}n_r\left(3 - n_r\right). \tag{S5}$$

Following similar steps, one can show that $\mathbf{S}_{r,1}^2 = 3/4$ and $\mathbf{S}_{r,2}^2 = 3/4$ are satisfied when written in terms of DFs. Therefore, Eq. (S1) has the final form,

$$\mathbf{S}_r^2 = n_r(3 - n_r), \tag{S6}$$

where $n_r = \sum_a f_r^{a\dagger}f_r^a$. The vacuum, singly, doubly, and fully occupied DF states are eigenstates of (S6) with eigenvalues 0,2,2, and 0, respectively.

The third component of the dimer spin, $S_r^z = (S_{r,1}^z + S_{r,2}^z)$, can be equivalently obtained by directly applying the DF mapping (2)-(3),

$$S_r^z = 2T_r^{xy}. \tag{S7}$$

Writing explicitly the number-conserving operator T in terms of DFs,

$$S_r^z = -\mathrm{i}(f_r^{x\dagger}f_r^y - f_r^{y\dagger}f_r^x). \tag{S8}$$

Applying the third component to the vacuum and doubly occupied states

$$S_r^z\,|000\rangle = 0, \tag{S9}$$
$$S_r^z\,|011\rangle = -\mathrm{i}\,|101\rangle, \tag{S10}$$
$$S_r^z\,|101\rangle = \mathrm{i}\,|011\rangle, \tag{S11}$$
$$S_r^z\,|110\rangle = 0 \tag{S12}$$

where we have used $|n^x, n^y, n^z\rangle$ with $n^a = f^{a\dagger} f^a$ $(a = x, y, z)$ to refer to the dimer states in terms of the DF occupation basis. Collecting the eigenvalues of the total spin (S6) and its third component we can unambiguously identify the vacuum with the singlet, $|s\rangle = (1/\sqrt{2})(|\uparrow\downarrow\rangle - |\downarrow\uparrow\rangle)$,

$$|000\rangle = |s\rangle\,, \tag{S13}$$

and $|110\rangle$ with the non-magnetic triplet, $|t_0\rangle = (1/\sqrt{2})(|\uparrow\downarrow\rangle + |\downarrow\uparrow\rangle)$,

$$|110\rangle = e^{\mathrm{i}\phi}\,|t_0\rangle\,, \tag{S14}$$

where ϕ is a phase to be determined below.

Diagonalizing the subspace defined by (S10) and (S11) we can identify the other two triplet states, $|t_+\rangle = |\uparrow\uparrow\rangle$ and $|t_-\rangle = |\downarrow\downarrow\rangle$, by

$$|t_+\rangle = \frac{e^{\mathrm{i}\varphi_+}}{\sqrt{2}}(-\mathrm{i}\,|101\rangle + |011\rangle), \tag{S15}$$

$$|t_-\rangle = \frac{e^{\mathrm{i}\varphi_-}}{\sqrt{2}}(\mathrm{i}\,|101\rangle + |011\rangle). \tag{S16}$$

where φ_+ and φ_- are phases that will be determined in the following by applying the non-conserving number operator Δ in terms of spin operators to the vacuum –i.e. the singlet state. In particular, by noticing that $|110\rangle = 2\mathrm{i}\Delta_r^{xy}\,|000\rangle$ and that $(S^z_{r,1} - S^z_{r,2}) = 2\Delta_r^{xy}$ we have that

$$|110\rangle = \mathrm{i}(S^z_{r,1} - S^z_{r,2})\,|s\rangle = i\,|t_0\rangle\,. \tag{S17}$$

Comparing with (S14), then $\phi = \pi/2$. Following analogous arguments and recalling that $S^x = (S^+ + S^-)/2$ and $S^y = (S^+ - S^-)/2\mathrm{i}$ where $S^\pm$ stand for the ladder operators of the SU(2) group,

$$|101\rangle = \frac{1}{\sqrt{2}}(|t_+\rangle + |t_-\rangle), \tag{S18}$$

$$|011\rangle = -\frac{\mathrm{i}}{\sqrt{2}}(|t_+\rangle - |t_-\rangle). \tag{S19}$$

Finally, inverting the relations we have

$$|s\rangle = |000\rangle\,, \tag{S20}$$

$$|t_0\rangle = -\mathrm{i}\,|110\rangle\,, \tag{S21}$$

$$|t_+\rangle = \frac{1}{\sqrt{2}}(|101\rangle + \mathrm{i}\,|011\rangle), \tag{S22}$$

$$|t_-\rangle = \frac{1}{\sqrt{2}}(|101\rangle - \mathrm{i}\,|011\rangle). \tag{S23}$$

Equivalently, the fully and singly occupied states comprise a second equivalent copy of the singlet and triplet states.

LOCAL HAMILTONIANS OF THE SVBC AND CVBC PARENT HAMILTONIANS

The parent Hamiltonian of a VBC can be written as a translational invariant sum of local Hamiltonians shifted by the DF vacuum eigenvalue, $H = \varepsilon + \sum_j H_j$, where $\varepsilon = -3J_x\mathcal{N}/8$. In particular, the local Hamiltonian corresponding to the sVBC parent Hamiltonian (12) is

$$H_j = \frac{3}{8}J_x + \frac{J_x}{2}B_{j,j+\hat{x}} + \frac{J_y}{2}B_{j,j+\hat{y}} + J_2(B_{j,j+\hat{x}+\hat{y}} + B_{j+\hat{x},j+\hat{y}}) + QB_{j,j+\hat{x}}B_{j+\hat{y},j+\hat{x}+\hat{y}}, \tag{S24}$$

that has a zero eigenvalue for $-4/3 \geq J_y/J_x \geq 2/3$ when the second-NN HB and four-spin interaction strengths are fixed to $J_2 = J_y/2$ and $Q = 2J_x/3$ respectively, as indicated in the main text.

The local Hamiltonian of the cVBC parent Hamiltonian (13) is

$$\begin{aligned} H_j = {} & \frac{3}{8}J_x + \frac{J_x}{4}B_{j,j+\hat{x}} + \frac{J_y}{3}B_{j,j+\hat{y}} + \frac{J_2}{2}(B_{j,j+\hat{x}+\hat{y}} + B_{j+\hat{x},j+\hat{y}}) \\ & + J_4(B_{j,j+2\hat{x}+\hat{y}} + B_{j+\hat{y},j+2\hat{x}}) + \widetilde{Q}_x(B_{j,j+\hat{x}}B_{j+\hat{x}+\hat{y},j+2\hat{x}+\hat{y}} + B_{j+\hat{x},j+2\hat{x}}B_{j+\hat{y},j+\hat{x}+\hat{y}}), \end{aligned} \tag{S25}$$

that has zero eigenvalue for $J_y = 0$ when the interactions are fixed to $J_2 = J_y$, $J_4 = J_y/2$, and $\widetilde{Q}_x = J_x/3$, as indicated in the main text.